

# APPLICATIONS BULLETIN

## Special Issue: Nano Tribometer Applications

### *Investigation of lubrication regimes using ultra low contact pressures*

Measurement of tribology at the micro and nano scales has been limited in recent years by the lack of dedicated instrumentation. The Scanning Force Microscope (SFM) has been the instrument of choice for investigating friction, wear and lubrication at such small scales. However, the SFM often produces contact pressures in the gigapascal range owing to the small dimensions of the tip. The recently developed Nano Tribometer allows a much greater variation in contact conditions, and is therefore more suited to the study of lubricants at very low loads. A recent study [1] has been able to show the transition through differing lubrication regimes as the applied load is varied on a lubricated contact.

The lubricants investigated were of two different types. The first was a mineral oil (MO) consisting of 3% aromatics, 31% naphthenes and 66% paraffins, with viscosities of 40 cSt, 96 cSt and 200 cSt. The second was a synthetic oil composed of polyalphaolefine (PAO) with a base viscosity of 6 cSt, to which two additives were added: The 'Irgalube 63' additive contains dithiophosphate and is used as an extreme pressure, anti-wear additive for industrial lubricants and greases. The 'Irgalube 211' additive contains alkylated triphenyl phosphorothionate and is used as an anti-wear additive in metal-working fluids and automotive engine oils.

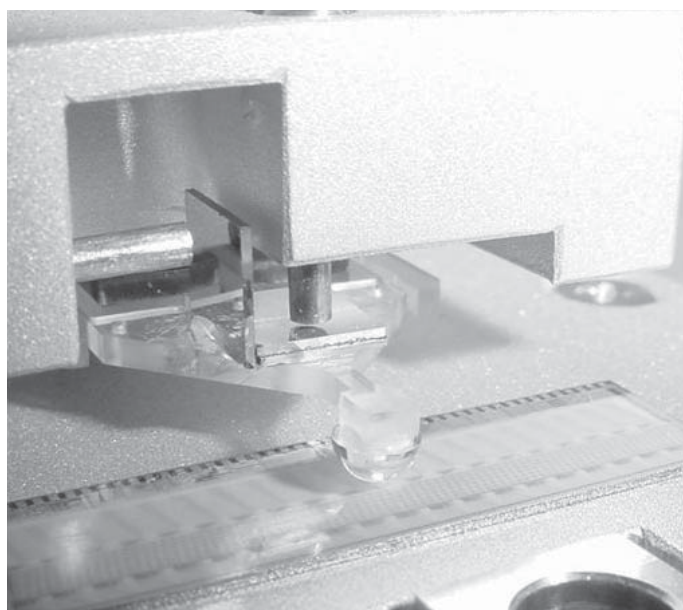


**Figure 1** : Close-up view of the Nano Tribometer glass spring force sensor which allows loading through the range 20  $\mu\text{N}$  - 1 N.

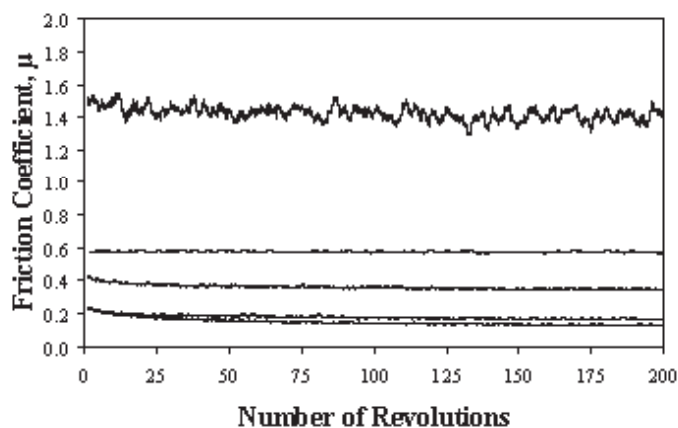


**Figure 2** : Experimentally measured friction coefficients as a function of rotational laps for a 200 cSt high purity mineral oil, for applied loads in the range 250  $\mu\text{N}$  - 25 mN.

In order to fully describe the interaction of two surfaces and an intermediary lubricant layer subjected to both normal and sliding forces, one must look at the definitions that describe not only the geometric and hydrodynamic parameters but also the elastic deformations that occur around the zone of interaction. Elastohydrodynamic lubrication (EHL) between a sphere and a flat plate can be described by a power law [2] which relates various parameters to the minimum lubricant film thickness ( $h_{\min}$ ) at the contact point:

$$h_{\min} = 1.79R^{0.47}\alpha^{0.49}\eta_0^{0.68}U^{0.68}E^{-0.12}W^{0.07}$$

where  $R$  is the radius of the spherical partner,  $U$  is the sliding velocity,  $W$  is the normal load and  $\alpha$  and  $\eta_0$  are lubricant properties relating the change of viscosity under increasing pressure.  $E$  is the reduced elastic modulus of the surface as described by Hertzian theory.

The Nano Tribometer tests were carried out using a 100Cr6 steel ball of diameter 2 mm as the spherical partner with a TiN-coated steel disk as the plate on which the test oils could be applied using a micropipette. Each test was performed with exactly 30  $\mu\text{l}$  of oil and the plate was rotated at a rate of 20 rpm giving an effective linear velocity of 4.2  $\text{mms}^{-1}$  at the point of contact. Seven constantly applied loads of 250  $\mu\text{N}$ , 500  $\mu\text{N}$ , 1 mN, 2 mN, 4 mN, 10 mN and 25 mN (which represent Hertzian contact pressures of approximately 110 MPa, 140 MPa, 180 MPa, 225 MPa, 280 MPa, 385 MPa and 520 MPa respectively) were used for each test cycle. The frictional force ( $F$ ) was measured over 200 revolutions of the plate and therefore the coefficient of friction ( $\mu$ ) could be calculated as  $\mu = F/W$ , with  $W$  representing the normal load as applied by the glass spring cantilever assembly (shown in Fig. 1).

A complete set of measured friction coefficient data for one of the test oils (200 cSt) is shown in Fig. 2 for the load range 250  $\mu\text{N}$  - 25 mN. It can be seen that as the load is increased, the interaction of the ball, sample surface and lubricant fall between three distinct regimes. For loads of 250  $\mu\text{N}$  and 500  $\mu\text{N}$  the lubricant inhibits the sliding motion of the ball on the surface leading to higher frictional resistance. At 1 mN, the friction coefficient is still high but the curve gradually decreases over the duration of the test, characteristic of the "running-in" of the surfaces. For loads greater than 2 mN, the curves seem to have a running-in period after which a steady state is reached where the coefficient of friction stabilises to a constant value.

The minimum lubricant film thickness can be calculated from the power law for various different oil viscosities, as shown in Fig. 3. The results here are shown as a function of normal load, although the equation shows that the sliding velocity and the sphere radius have a much more significant influence on the film thickness than the applied load.

The power law equation shows that for any given ball-on-flat system, decreases in normal load or increases in sliding speed lead to increases in the lubricant film thickness. At some point the film thickness will be so great as to completely separate the surface asperities of the two opposing surfaces. Such a condition is referred to as *full film* or hydrodynamic lubrication and, because there is no longer any interaction between mating material surfaces, the lubricant film thickness becomes governed by the viscosity, speed and normal load.

An exponential increase in the friction coefficient is shown in Fig. 4 (a) as the film thickness increases. This behaviour is evident for all four viscosities plotted. For low loads where the Hertzian contact pressures fall to around 110 MPa, the friction is at a maximum. As the load is subsequently increased, the friction decreases (seen as the initial decrease of each curve). In the cases of the 40 cSt and 96 cSt viscosities, it is clearly visible that there is an optimum film thickness/normal load which causes a minimum friction coefficient.

The transition between different lubrication regimes can be seen if the coefficient of friction is plotted as a function of the *Stribeck* number,  $L$ , where  $L = \eta U/W$ . The results for the same four viscosities are shown in Fig. 4 (b) where the transition from elastohydrodynamic to hydrodynamic regimes can clearly be seen. In order to investigate the boundary lubrication regime, a much lower sliding speed would be required at the contact. At such low speeds, there is no pressure build-up in the lubricant and therefore the load is totally carried by the asperities in the contact area.

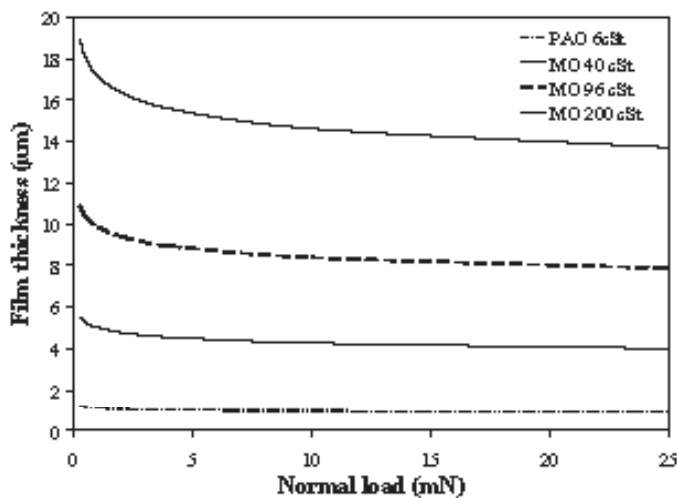


**Figure 3** : Calculated oil film thicknesses as a function of normal load for four different oil viscosities (sphere radius of 1 mm).

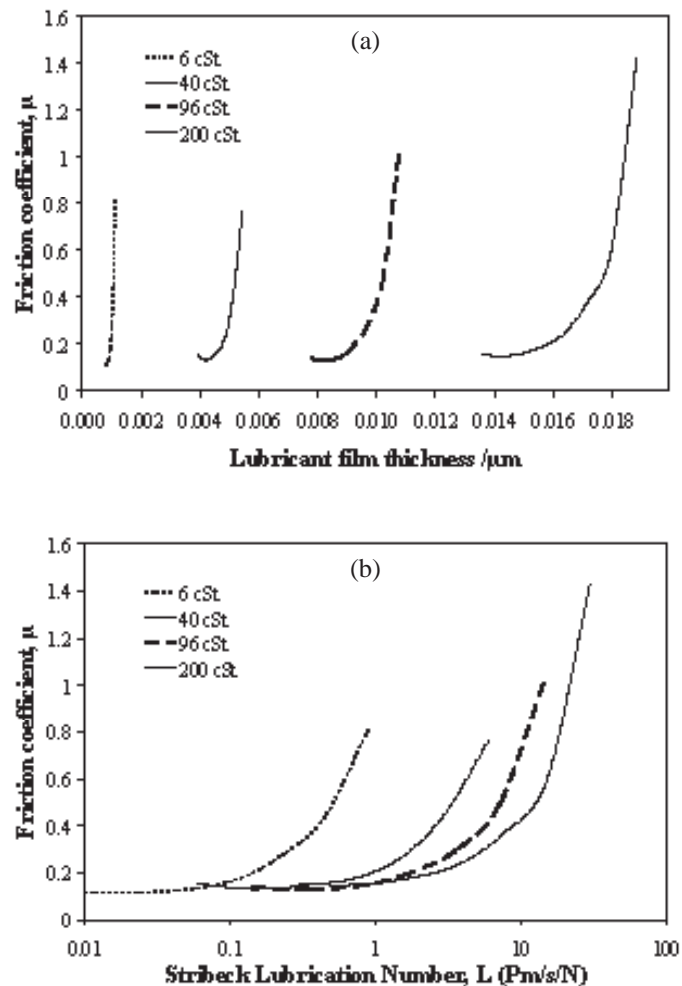


**Figure 4** : Experimental results for the friction coefficient of a 100Cr6 ball of radius 1 mm in contact with a TiN-coated steel sample. Sliding velocity was 4.2  $\text{mms}^{-1}$  and four different oil viscosities are shown. The film thickness is plotted in (a) whereas a Stribeck representation is given in (b).

Although the Nano Tribometer is ideally suited to the characterisation of lubricant properties at the micro and nano scales, it can also be of interest to correlate such results with measurements made at the macro scale on a different instrument. By using three different instruments it has been possible to map the three lubrication regimes of a 200 cSt mineral oil. A standard pin-on-disk machine was used to measure the friction coefficient from the boundary condition with  $\mu$  being initially stable at around 0.3 (for  $L$  values of 0.15 - 1) after which it drops to a minimum  $\mu$  of 0.11 (at  $L = 20$ ). The Nano Tribometer is then used to measure  $\mu$  from  $L$  values of about 10 up to 5000. This covers the transition from mixed to hydrodynamic regimes (contact conditions are radius of 1 mm and sliding velocity 4.2  $\text{mms}^{-1}$ ).

For higher sliding speeds, the Nano Scratch Tester is used with a contact radius of 20  $\mu\text{m}$  and a sliding velocity of 1  $\text{cms}^{-1}$ . This allows  $\mu$  to be measured up to an  $L$  value of around 70'000. This is a good example of how the measurement capabilities of three instruments can be combined to give frictional information from the macro down to the micro scales.

[1] R. A. J. Soden, *Microtribological investigation into elastohydrodynamic and hydrodynamic lubrication regimes using ultra low contact pressures*, Tribotest (2004) in press

[2] I. M. Hutchings, *Tribology: Friction and wear of Engineering Materials*, Butterworth-Heinemann, Fifth Edition (2001)

# Adhesion and friction studies of materials for microelectromechanical systems (MEMS)

Because of the large surface area to volume ratio in MEMS devices as the size scale decreases, the surface forces such as adhesion and friction become increasingly critical and dominate over inertial and gravitational forces. This application note presents some results [1] from measurements made with a Nano Tribometer on a selection of commonly used MEMS structural materials.

The tests were performed using a Si (100) ball of radius 500  $\mu\text{m}$  as the spherical partner mounted on a stainless steel cantilever. The three sample materials consisted of a single-crystal Si (100) wafer (phosphorous doped), a diamond-like carbon (DLC) film of thickness 10 nm (deposited on a Si (100) wafer) and a hexadecane thiol (HDT) self-assembled monolayer (SAM) deposited on a Au(111)/Si(100) substrate by immersion.

The adhesive forces were measured in ambient conditions (22°C, relative humidity of 45% - 55%) using a technique very similar to the 'force calibration plot' method used in Scanning Force Microscopy (SFM). This consists of bringing the ball into contact with the sample material in a controlled way and keeping the surfaces in contact for a period of time. The maximum force, needed to pull the upper and lower surfaces apart, is measured as the adhesive force.

A typical example of such an adhesion measurement is shown in Fig. 1 for a Si (100) ball in contact with a flat of the same material. As the ball approaches the flat sample within a few nanometers (point A), an attractive force exists between the two surfaces. The ball is therefore pulled toward the sample and contact occurs at point B. The adsorption of water molecules on the sample surface can also accelerate this so-called *snap-in*, due to the formation of a water meniscus. From this point on, the ball is in contact with the sample surface, and as the Z-piezo extends further, the cantilever is further deflected. This is represented by the sloped portion of the curve. The time effects on the adhesive force can be studied by maintaining the Z-piezo at its maximum length for various time periods. As the ball is then retracted from the surface (point C), it goes beyond the zero deflection (flat) line due to the attractive force. This phenomenon can be due to long-range meniscus force, van der Waals force or electrostatic force. At point D, the ball snaps free of the adhesive forces and is again in free air.

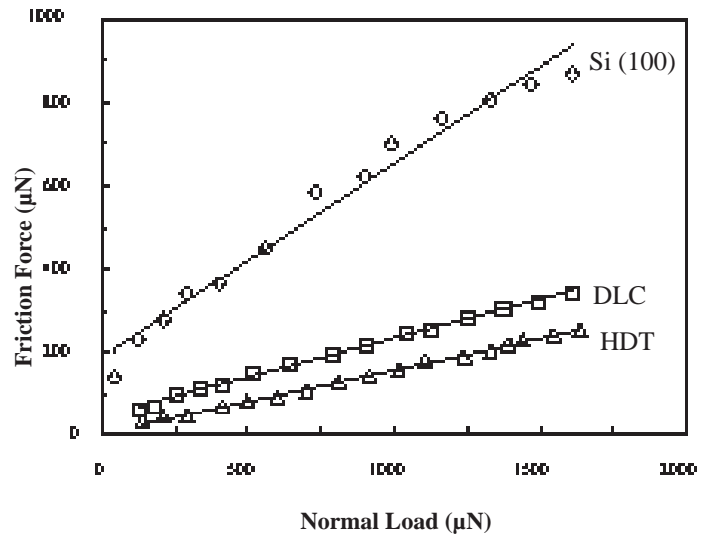
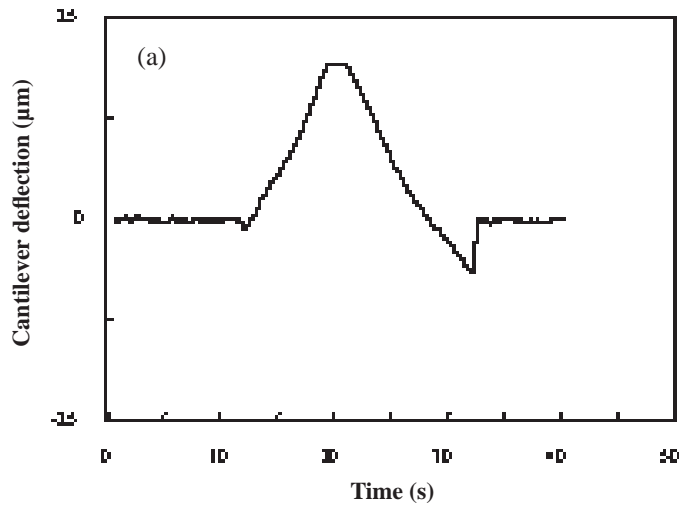


Figure 2: Friction force as a function of normal load for measurements made on Si (100), DLC and HDT surfaces with a Si (100) ball of radius 500  $\mu\text{m}$ . A sliding speed of 720  $\mu\text{m/s}$  and sliding amplitude of 1000  $\mu\text{m}$  were used in the linear reciprocating mode.

The frictional forces were measured by using the instrument in the linear reciprocating mode (as opposed to the pin-on-disk mode) with applied normal loads in the range 100 to 2500  $\mu\text{N}$ . Average values of the coefficient of friction were obtained by measuring the frictional force as a function of normal load and reproducibility was found to be within  $\pm 5\%$ . Some typical results are summarised in Fig. 2 where it can be seen that all three samples exhibit a linear response over the measured load range. The coefficients of friction were calculated and ranked in the following order:  $\mu_{\text{Si}} (0.47) > \mu_{\text{DLC}} (0.19) > \mu_{\text{HDT}} (0.15)$ . This confirmed that thin layers of DLC and HDT can be used as effective lubricants for Si materials in MEMS devices.

The effects of velocity were investigated by measuring the frictional force with velocities from 50 to 2200  $\mu\text{m/s}$ . All tests were carried out in an ambient condition at a normal load of 2000  $\mu\text{N}$ . The results are shown in Fig. 3 (a) and indicate that for Si (100), the friction force initially decreases until equilibrium occurs, whilst it seems that the velocity has almost no effect on the friction properties of DLC and HDT.

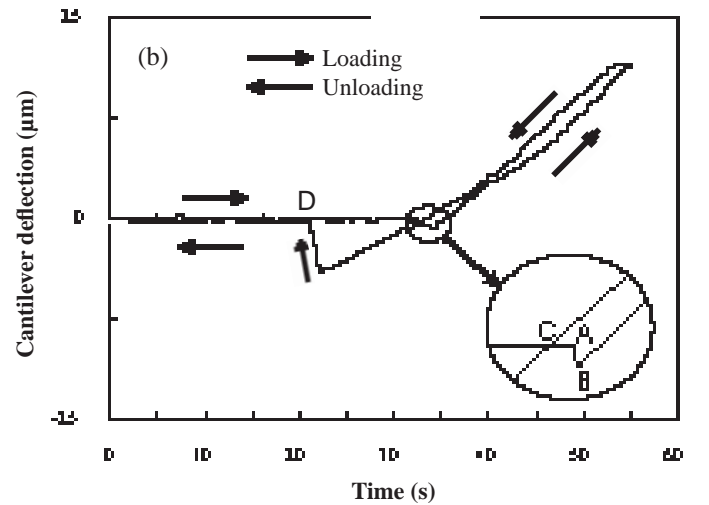
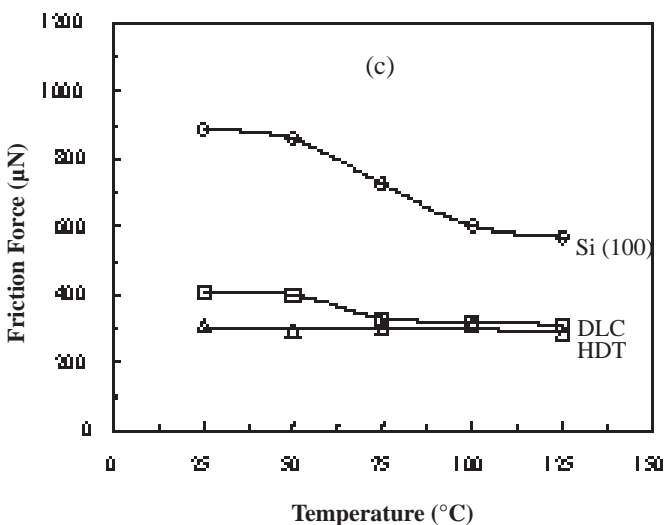
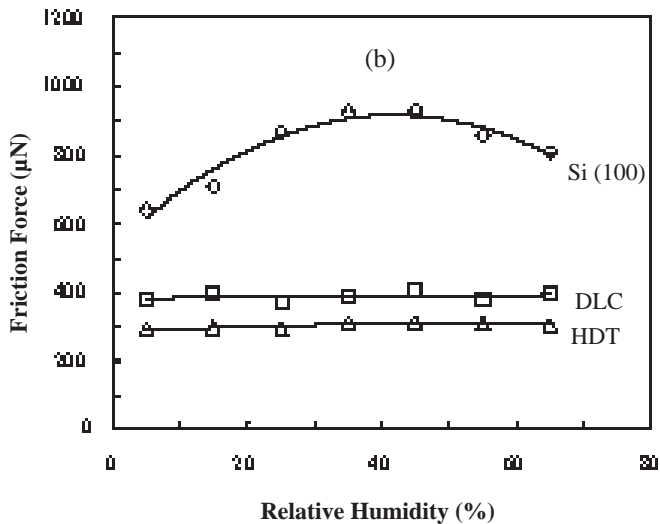
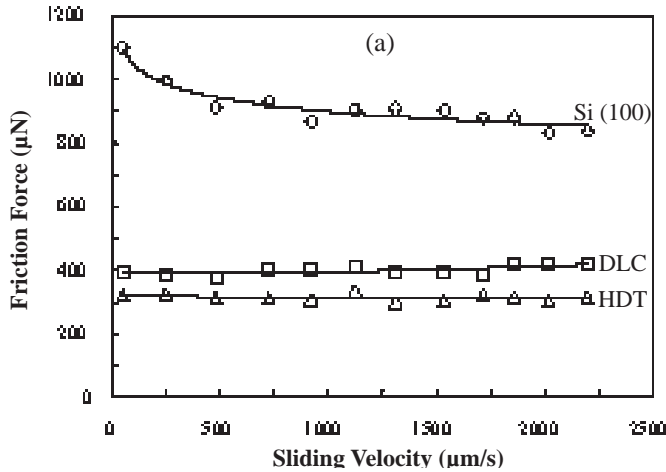


Figure 1 : Typical adhesion data for a Si (100) ball contacting a Si (100) flat with a rest time of 2 seconds. The cantilever deflection is plotted as a function of time (a) and of displacement (b) as the ball is approached to the surface, contact established and the ball then retracted.

For Si (100), at high velocity, the water meniscus is broken and does not have enough time to rebuild. Tribochemical reactions are also thought to play an important role, as the  $\text{SiO}_2$  native oxide interacts with water molecules producing  $\text{Si}(\text{OH})_4$  which is removed and continuously replenished during sliding. This  $\text{Si}(\text{OH})_4$  layer is known to be of low shear strength. On the other hand, the DLC and HDT surfaces exhibit hydrophobic properties and can only absorb a few water molecules in ambient conditions so the friction force is not significantly influenced by the sliding velocity.



velocity, (b) relative humidity and (c) temperature on the friction force of Si (100), DLC and HDT.

The effects of relative humidity were investigated by introducing a mixture of dry and moist air. The humidity could therefore be varied from 5% to 65% while the temperature, normal load and scanning velocity were maintained at 22°C, 2000 µN and 720 µms<sup>-1</sup> respectively. The results are shown in Fig. 3 (b) and it can be seen that for Si (100), the friction force increases with a relative humidity increase up to 45% but then shows a slight decrease with a further increase in the relative humidity. The humidity seemed not to have any influence on the friction properties of DLC or HDT. In the case of Si (100), the initial increase in humidity up to 45% causes more adsorbed water molecules which form a larger water meniscus which leads to an increase in friction. But at very high humidity (65%), large quantities of such molecules can form a continuous water layer which separates the ball and sample surfaces, creating a lubricant layer which causes a decrease in friction.

The temperature of the tribological contact was varied from 25°C up to 125°C whilst maintaining the relative humidity, normal load and scanning velocity at 45% - 55%, 2000 µN and 720 µms<sup>-1</sup> respectively. The results presented in Fig. 3 (c) show that at temperatures above 50°C, an increase in temperature causes a significant decrease in the friction for Si (100) and a slight decrease in the case of DLC. The HDT seems not to be influenced by changes in temperature over the range tested. At high temperatures, desorption of water and reduction of surface tension lead to the decrease in friction forces of Si (100) and DLC. However, in the case of HDT, only a few water molecules are adsorbed on the surface so the aforementioned mechanisms do not exert a significant influence and thus the HDT seems unaffected by any temperature change.

Dr Huiwen Liu and Prof. Bharat Bhushan of the Nanotribology Laboratory for Information Storage and MEMS/NEMS at Ohio State University are acknowledged for providing the results presented. Prof. Bhushan can be contacted at bhushan.2@osu.edu

[1] H. Liu and B. Bhushan, J. Vac. Sci. Technol. A 21 (4) (2003) 1528-1538



CSM Instruments Application Bulletins feature interesting applications of our full range of mechanical surface testing instruments and can be viewed on the CSM Instruments website.

Editor Dr. Nicholas X. Randall

Should you require further information, then please contact:

CSM Instruments	Tel: + 41 32 557 5600
Rue de la Gare 4	Fax: +41 32 557 5610
CH-2034 Peseux	instruments@csm-instruments.com
Switzerland	www.csm-instruments.com

DISTRIBUTOR: